

Intramolecular Charge Transfer Reaction, Polarity, and Dielectric Relaxation in AOT/Water/Heptane Reverse Micelles: Pool Size Dependence

Ranjit Biswas,^{*,†} Nashiour Rohman,^{‡,§} Tuhin Pradhan,[†] and Richard Buchner[‡]

Department of Chemical, Biological and Macromolecular Sciences, and Unit for Nanoscience and Technology, S. N. Bose National Centre for Basic Sciences, JD Block, Sector III, Salt Lake, Kolkata 700 098, India, and Institute of Physical and Theoretical Chemistry, University of Regensburg, D-93040 Regensburg, Germany

Received: March 17, 2008; Revised Manuscript Received: May 24, 2008

Intramolecular charge transfer (ICT) reaction in a newly synthesized molecule, of 4-(1-morpholenyl) benzonitrile (M6C), in AOT/water/heptane reverse micelles at different pool sizes has been studied by using steady-state and time-resolved fluorescence emission spectroscopy. The pool size dependences of the reaction equilibrium constant and reaction rate have been explained in terms of the average polarity of the confined solvent pools estimated from the fluorescence emission Stokes shift of a nonreactive probe, coumarin 153, dissolved in these microemulsions. The complex permittivity measurements in the frequency range $0.01 \leq \nu/\text{GHz} \leq 2$ for these microemulsions at different pool sizes ($0 \leq w_0 \leq 40$) and AOT concentrations ($0.1 \leq c/M \leq 0.5$) at 298.15 K have also been performed. At sufficient water content, a large dispersion with a relaxation time of ~ 600 ps has been observed at ~ 300 MHz and attributed to the average reorientation of water molecules residing in the close vicinity of the polar interface of the AOT headgroup and *n*-heptane. The reorientation of these interfacial water molecules is probably responsible for the nanosecond component observed in numerous polar solvation dynamics experiments in these reverse micelles. Subsequently, the estimated polarity and the measured reorientational time scale have been used to explain the dramatic slowing down of the ICT reaction rate and its dependence on pool size in these confined environments.

I. Introduction

Inverted or reverse micelles made of surfactant (charged or neutral), oil, and a polar solvent (not any polar solvent) are clear, homogeneous, and thermodynamically stable solutions.^{1–41} In such multicomponent mixtures, polar solvent molecules are trapped in a confinement created by the self-aggregation of the surfactant head groups, while the alkyl chain (“tail”) of the surfactant molecules remains immersed in the bulk nonpolar solvent (oil). Interestingly, surfactants with neutral or charged head groups³⁵ or even a mixture of surfactants with suitable combinations of polar and nonpolar solvents in the presence of a cosurfactant⁴² have also been found to form reverse micelles. The anionic surfactant sodium bis(2-ethylhexyl)-sulfosuccinate (AOT) forms reverse micelles in the presence of water and a nonpolar solvent (usually isooctane or heptane). In dilute aqueous solutions of AOT, the reverse micelle droplets are known to be spherical, and the radius of the trapped water pool is given by $r^{(0A)} \approx 2w_0$, where w_0 denotes the ratio between the molar concentration of water and the surfactant.^{5,35} Since water in tiny volume plays a crucial role as a medium that controls the function and dynamics near biological membranes and active biomolecular surfaces, reverse micelles typify a biological model of a living cell. They are also promising candidates for synthesis of nanoparticles, drug transportation to a specified position, and the subsequent delivery.

As the confinement severely affects the structure (mainly the H-bond network) of water molecules and considerably modifies

several bulk solvent properties such as static dielectric constant, viscosity, and compressibility, extensive research has been carried out over the years to understand the effects of surfactant–water interactions on the structure and dynamics of the encapsulated water molecules.^{1–43} Experimental^{1–3} and computer simulation^{27–29} studies have revealed that the long time component of polar solvation energy relaxation is ~ 1000 times slower than that observed in bulk water and also shows a pool size dependence. Vibrational echo studies of water in nanosized droplets have indicated the presence of a significant ultrafast component with a time constant of 30–50 fs in the decay of the frequency autocorrelation function.²⁶ Similar ultrafast decay has been either observed or estimated in solvent pools of quaternary microemulsions,⁹ lecithin vesicles,¹⁶ and catanionic reverse micelles.⁴² Recently, photoinduced intramolecular charge transfer (ICT) reaction has been studied in aqueous and several nonaqueous AOT/heptane reverse micelles where the importance of the reverse micelle interface to control a ICT process is stressed.^{40,41} However, no attempt, even at the semiquantitative level, has been made so far to correlate the rate and yield of a reaction that possesses an activation barrier occurring in these “nanoreactors” with the average polarity and dynamics of the confined pool. In this article we report such a study where photoinduced ICT reaction has been investigated in AOT/water/heptane reverse micelles at different pool sizes. As the polarity of a reaction medium plays a very important role in determining both the yield and the rate of a twisted ICT (TICT) reaction,^{43–45} we have made a continuum model estimate of the average polarity (in terms of static dielectric constant, ϵ_0) of the nanoconfinements in these microemulsions by following the steady-state fluorescence emission of a nonreactive solvation probe.⁴⁶ In addition, dielectric relaxation studies have been carried out to correlate the slowing down of the reaction rate

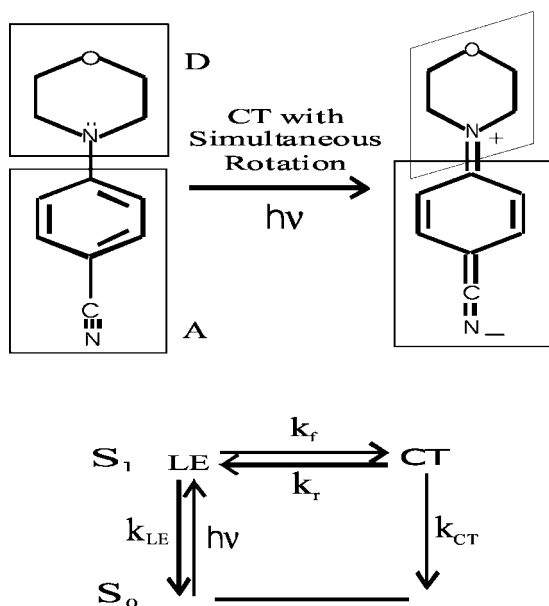
* Corresponding author. E-mail: ranjit@bose.res.in.

[†] S. N. Bose National Centre for Basic Sciences.

[‡] University of Regensburg.

[§] Presently at Chemistry & Physics of Materials Unit, Jawaharlal Nehru Centre for Advanced Scientific Research, Jakkur, Bangalore-560 064, India.

SCHEME 1



with the “slow” orientational dynamics of the polar environment trapped inside these microemulsions.

The molecule that we have used for studying the ICT reaction is 4-(1-morpholenyl) benzonitrile and is designated as M6C in Scheme 1. The structural similarity between M6C and 4-(1-piperidinyl) benzonitrile (P6C) molecules^{43–45} have led us to assume that the photoinduced charge transfer reaction in M6C in polar media also occurs simultaneously with the twisting of the morpholenyl group around the central bond joining the benzonitril moiety. Therefore, the photoinduced charge transfer reaction in M6C may be termed as a twisted intramolecular charge transfer (TICT) reaction. As shown in Scheme 1, photoexcitation promotes M6C to the locally excited (LE) state in the first excited electronic surface (S_1), which is relatively less polar and possesses charge distribution similar to that in the ground state. The photoprepared LE state then either undergoes ICT with the forward reaction rate k_f or comes back to the ground (S_0) state with an average (radiative + nonradiative) rate (k_{LE}). Likewise, the charge transferred (CT) state can go back to the LE state with a rate of k_r or populates the ground state via the radiative and nonradiative pathways with the average rate, k_{CT} . The activation barrier that separates the LE state from the more polar CT state is expected to be $\sim 5k_B T$,⁴⁵ where $k_B T$ denotes the Boltzmann constant times the absolute temperature. Since time scales in such low barrier reactions are typically in the picoseconds,⁴⁷ the slow solvent modes with a nanosecond time scale observed in these reverse micelles means that the reaction may occur even before the solvent reorganization is complete. In addition, the drastically reduced average dielectric constant of the nanopool decreases the changes in reaction free energy ($-\Delta G_T$) by substantially reducing the equilibrium constant (K_{eq}) for the $LE \rightarrow CT$ conversion reaction. Since interactions with the surfactant head groups render the nanoenvironment more rigid than the bulk polar solvent,^{2,3} the twisting mode involved in the $LE \rightarrow CT$ conversion reaction is also expected to experience more retardation. This, in turn, would reduce the rate of such a reaction. The reduction in dielectric constant, on the other hand, reduces the dielectric contribution to the total friction and hence assists the twisting. All these factors, therefore, lead to complicated environment effects on TICT reaction rate in reverse micelles.

The present paper reports the following results. Quantum yield and radiative rate are found to decrease with the pool size, whereas the changes in reaction free energy and the nonradiative rate increase with the size of the reverse micelles. As expected, the formation of the CT state increases with pool size, and the peak frequency of the CT emission band shifts toward lower energy. The time-resolved emission decays of M6C have been analyzed by using the kinetic framework employed earlier for studying the TICT reaction of several substituted benzonitril derivatives in normal solvents,⁴⁵ liquid mixtures,^{48–50} and electrolyte solutions.^{51,52} Note that the emission decay of M6C in heptane at several wavelengths across the emission band has been found to be single exponential with only one time constant of approximately 2 ns, which is very similar to the decay characteristic of the closely related compound P6C in several nonpolar solvents.⁴⁵ For all pool sizes, the emission decay of M6C collected near the LE peak wavelength is found to be a biexponential function of time with shorter and longer decay time constants. At a few pool sizes for which the CT emission decay could be collected,⁵³ the decay is characterized by a rise component (negative amplitude) associated with a shorter time constant (of the two time constants) and a longer decay time constant. Also, the time constant associated with fast component of the LE decay is found to be very similar with the risetime constant of the CT decay. The shorter time constant is identified with the reaction time for the $LE \rightarrow CT$ conversion reaction in M6C, which decreases by a factor of 2 as the pool size swells up by a factor of 33. Most importantly, the reaction time in these confinements is in the range of 200–400 ps, which is 10–20 times slower than that for M6C in the moderately polar ($\epsilon_0 \sim 10$) bulk solvents. The estimated dielectric constant at the largest pool size ($w_0 \approx 37$) is found to be ~ 4 times less than that of the bulk water. The dielectric relaxation measurements in these microemulsions at 0.5 M AOT indicate the presence of a Cole–Davidson-type relaxation process with time constants in the range of 500–800 ps. This orientation relaxation time scale is therefore well-correlated with the slow reaction time scales (200–400 ps) found in the AOT/heptane/water reverse micelles.

The organization of the rest of the article is as follows. Experimental details are discussed in Section II, followed by results and discussion in Section III. Concluding remarks are given in Section IV.

II. Experimental Details

M6C was synthesized by following the protocol given in the literature.^{54,55} Approximately 1.5 g (12 mmol) of 4-fluorobenzonitrile (Alfa Aesar, 99%) and the triple molar quantity of morpholine (4 g, 46 mmol) (LOBA CHEMIE, India) were dissolved in 25 mL of dimethyl sulfoxide (Aldrich) and stirred in refluxed conditions for 24 h at 365 K. The mixture was then cooled and poured into 500 mL water (Millipore), and the product separated by filtration was dried and recrystallized three times from cyclohexane (Merck, Germany). Purity of the compound was checked by thin layer chromatography and monitoring the excitation wavelength dependence of fluorescence emission in several bulk polar and nonpolar solvents.

AOT ($\geq 98\%$, Fluka, Switzerland, purum, and Sigma, $\geq 99\%$) was used after vacuum drying for 24 h. Spectroscopic grade *n*-heptane (Merck, $\geq 99.5\%$) was used after drying over molecular sieves and filtration. Laser grade coumarin 153 (C153) was purchased from Exciton and used as received. Solutions were made by dissolving a measured amount of solid AOT in *n*-heptane (heptane hereafter) by volumetric method. Subse-

quently, deionized water (Millipore) was added to the solution to obtain appropriate w_0 , where w_0 denotes the ratio of molar concentration of water to AOT. The concentration of AOT in all reverse micelles was maintained at 0.1 M. The mixtures were then gently stirred to obtain transparent, homogeneous, and thermodynamically stable solutions.

Steady-state absorption and emission spectra were recorded respectively by using a spectrophotometer (Shimadzu, UV-2450) and a fluorimeter (SPEX fluoromax-3, Jobin-Yvon, Horiba). The solute concentration was maintained at a sufficiently dilute concentration ($\leq 10^{-5}$ M) by adjusting the absorbance of the sample to ~ 0.1 . For a given sample, the peak wavelength (λ) of the absorption spectrum was used as the excitation wavelength for the corresponding emission scan. The fluorescence emission spectra were suitably corrected and background subtracted for further processing. Note that all the spectroscopic studies reported here were carried out by using only one excitation wavelength corresponding to the peak of the absorption spectrum, even though these systems are microscopically heterogeneous and show excitation wavelength dependence.^{1-3,42} A few samples were bubbled with dry argon gas, which produced very little or no effects on the overall appearance of the spectra for C153 and M6C in solutions and also on the decay kinetics for the TICT molecule. We used the emission peak frequency versus dielectric field factor correlation curve^{56,57} in order to estimate the average dielectric constant of the polar pool from the emission of C153 dissolved in these microemulsions.

The equilibrium constants (K_{eq}) and the change in reaction free energy ($-\Delta G_r$) for the LE \rightarrow CT conversion reaction in M6C were then determined from the area under the LE and CT bands obtained after deconvolution of the full emission spectrum of M6C in a given microemulsion into two fragments by using the reference emission spectrum of M6C in perfluorohexane.^{45,50,51} Algebraic addition of the shifts of the emission spectra from the peak of the reference emission spectrum to the *average* peak frequency of the reference emission spectrum then provided the emission peak frequencies of the LE and CT bands. The *average* of the reference emission peak frequency was calculated by averaging the numbers obtained by fitting the upper half of the reference emission spectrum with an inverted parabola, the first moment, and the arithmetic mean of the frequencies at half-intensities on both blue and red ends of the emission spectrum.^{56,57} Absorption peak frequencies were obtained by calculating the first moments of the absorption spectra. The error associated with the peak frequency determination is typically ± 250 cm^{-1} , and that associated with the band area is $\sim 10\%$ (of the reported value). Lifetime data for measuring radiative and nonradiative rates and time-resolved fluorescence emission intensity decay data for M6C in microemulsions were collected by using a time-correlated single photon counting apparatus (Lifespec, Edinburgh Instruments) with excitation wavelengths at 299 nm and an emission band-pass of 8 nm. The full width at half-maximum of the instrument response function (IRF) was ~ 475 ps. The emission decay collected at magic angle was then deconvoluted from the IRF and fitted to the multiexponential function of time using an iterative reconvolution algorithm.⁴⁵ For a few samples, emission decays collected at wavelengths near the peak and at half-intensities on both the blue and red ends of the LE emission band. These decays were found to fit globally to a biexponential function of time with short and long time constants.⁵⁸

The total complex permittivity, $\epsilon^*(\nu) = \epsilon'(\nu) - i\epsilon''(\nu)$ of the samples were measured by using a time domain reflectometer, where $\epsilon'(\nu)$ and $\epsilon''(\nu)$ respectively denote the relative permit-

tivity and dielectric loss of the solutions. The technique covers the frequency range of $\sim 0.01 \leq \nu/\text{GHz} \leq 2$.^{59,60} $\epsilon''(\nu)$ is obtained from the experimentally accessible total loss, $\eta''(\nu)$, by using the relation $\epsilon''(\nu) = \eta''(\nu) - \kappa/2\pi\nu\gamma_0$, where κ is the specific conductivity of the solution, and γ_0 is the vacuum permittivity. The uncertainty in the measurements of $\epsilon'(\nu)$ and $\eta''(\nu)$ relative to the static permittivity of the sample is within $\pm 2\%$. The electrical conductivity measurements of the solutions were done by using a Consort Ion/EC Meter C733 equipped with platinum electrodes calibrated with 0.1 M KCl solutions.⁶⁰ All the measurements reported here were performed at $T(\text{K}) = 298.15 \pm 0.05$.

III. Results and Discussion

A. Estimation of the Average ϵ_0 of the Confined Pool. As the polarity of a medium plays a dominant role in controlling the yield as well as the rate of a TICT reaction, one would like to know the average dielectric constant (ϵ_0) of the polar solvent pools inside the microemulsion droplets at various water concentrations. The following empirical relation is used to estimate the average ϵ_0 of the solvent pools from the emission peak frequency (ν_{em}) of C153 dissolved in these microemulsions:⁵⁶

$$\nu_{em} (10^3 \text{ cm}^{-1}) = 23.12 - 5.06[(\epsilon_0 - 1)/(\epsilon_0 + 2)] - 1.5[(n^2 - 1)/(n^2 + 2)] \quad (1)$$

where n denotes the refractive index of the solvent. Note that the above empirical relation and similar ones (for anthracene and its substituted derivatives) have previously been found^{57,61} to be successful in semiquantitative estimation of the local density around an attractive solute in supercritical fluids. Here we assume the refractive index of the trapped pool as that of bulk water. A simple numerical inversion of the above relation with a given value of ν_{em} then provides an estimate of the average ϵ_0 . Note that, for these microemulsions, the estimated value of ϵ_0 corresponding to a value of ν_{em} is *not* a unique one, as the latter (emission peak frequency) shows excitation wavelength dependence in these microscopically heterogeneous systems.^{1-3,35} Nevertheless, this approach provides a qualitative understanding of the confinement effects on the medium polarity and could be useful for assessing the pool-size-dependent environment effects on a chemical reaction. The values of ϵ_0 estimated by using eq 1 are shown as a function of pool size (w_0) in Figure 1. Representative emission spectra of C153 in AOT/water reverse micelles at several pool sizes are provided in the Supporting Information (Figure S1). It is evident from Figure 1 that the bulk dielectric constant of water decreases drastically upon confinement, which has also been predicted by a recent simulation study.⁶² Also note that the dielectric constant of the confined pool increases as the size of the pool grows upon addition of water. At $w_0 \approx 37$, the dielectric constant is almost one-third that of bulk water.

The drastic reduction of the dielectric constant upon confinement may be connected to the substantial slowing down of the polar solvation dynamics in AOT/water reverse micelles^{1-3,6-10} as follows. The curvature of the potential energy surface in which the polar solvation energy relaxes is determined by the longitudinal component of the wavevector (k)-dependent static dielectric constant $\epsilon_L(k)$ at its long wavelength limit.^{63,64} As ϵ_0 decreases, the curvature becomes flatter, and consequently the relaxation becomes slower. Therefore, the solvent dynamics in response to a photoexcited probe becomes slower in AOT/water reverse micelles on *at least* two counts: they are the reduction

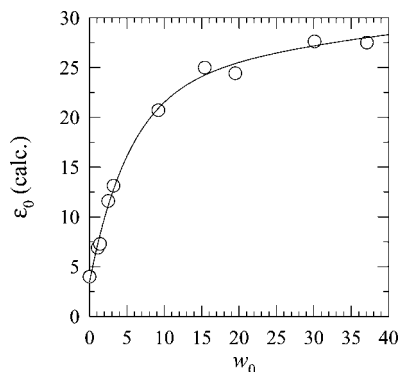


Figure 1. Estimated values of static dielectric constant (ϵ_0) at different pool sizes (w_0) as reported by the peak frequencies of the emission spectra of a nonreactive solvation probe in AOT/water/heptane reverse micelles. The pool size is controlled by varying the water concentration at a particular surfactant concentration (here AOT) in the microemulsion. That is, $w_0 = [\text{water}]/[\text{AOT}]$.

of ϵ_0 and the sluggish movements (both rotational and translational) of the solvent molecules due to the increase in microviscosity (or rigidity) upon confinement. Interestingly, however, the dramatic slowing down of the long time component (~ 1000 times slower than in bulk water) observed in the Stokes shift dynamics is absent in the vibrational echo decays and vibrational echo peak shift measurements.^{25,26} Vibrational echo experiments report a pool-size-dependent dynamics and, most importantly, reveal that the long time dynamics in the smallest pool is slowed down by a factor of 10 only, even though a large ultrafast component with a time constant of ~ 40 fs is found to be present in the frequency–frequency correlation function (FFCF).²⁶ Simulation studies have interpreted the slow solvent dynamics in terms of electrostatic ion–solvent interactions,^{27,28,65} although the echo experiments²⁶ assert that the geometric confinement rather than the ionic strength is responsible for the sluggish movement of the solvent particles inside the microemulsions. We therefore believe that the flattening of the surface curvature due to the drastic reduction of the average dielectric constant of water in concert with the slower solvent orientational relaxation renders the dielectric response of the solvent to an excited solute probe ~ 1000 times slower in confined environments than that in the bulk. Subsequently, the modified solvent dynamics contributes to the slowing down of a TICT reaction occurring inside the reverse micelles.

B. Estimation of the Solvent Orientational Relaxation Time Scale in the Confined Pool. The frequency (ν)-dependent real, $\epsilon'(\nu)$, and loss, $\epsilon''(\nu)$, components of the complex permittivity of AOT/water/heptane reverse micelles are analyzed simultaneously with various conceivable relaxation models by using a least-squares technique.⁶⁶ The experimental permittivity has been fitted to the following general function:

$$\epsilon^*(\nu) = \epsilon_\infty + \frac{\epsilon_0 - \epsilon_\infty}{[1 + (j2\pi\nu\tau)^{1-\alpha}]^\beta} \quad (2)$$

where the observed dispersion is attributed to only one single step, with ϵ_∞ as the infinite (or optical) frequency dielectric constant, τ as the relaxation time, and $j^2 = -1$. α and β are two constants that define several relaxation processes. For example, the Cole–Davidson (CD) process corresponds to $\alpha = 0$ and $0 < \beta \leq 1$; the Cole–Cole (CC) process corresponds to $\beta = 1$ and $0 < \alpha \leq 1$, and the Debye (D) process corresponds to $\alpha = 0$ and $\beta = 1$.⁶⁷ Note that the measurements were done at w_0 values avoiding the steep rise in the specific conductivity, κ (see Figure S2, Supporting Information).

Figures S3 and S4 in the Supporting Information suggest that a dispersion step at ~ 300 MHz exists for solutions containing sufficient amounts of water. A solution containing 0.5 M AOT and no water (that is, $w_0 = 0$) does not show any dispersion at ~ 300 MHz. This indicates that the observed dispersion might be due to the reorientation of water molecules residing in the close proximity of the polar interface in the reverse micelles.⁶⁸ The dielectric relaxation parameters obtained after fitting the permittivity data for various w_0 values at 0.5 M AOT are summarized in Table 1. The goodness of fit parameter (χ^2) shown in the table (Table 1) obtained after considering both the Cole–Davidson and Debye processes suggest that both of the processes seem to describe the relaxation processes reasonably well. Note that the data for reverse micelles that contain 0.1 M AOT are not included, as permittivity measurements did not signal any relaxation processes within the experimental window for these samples. It may be that, for dispersion to be observed in microemulsions, a sufficient amount of water molecules should be present in the system.⁶⁹

Note that the time scale (τ values) for w_0 values ranging from 10 to 40 at an AOT concentration of 0.5 M is lying in the range of 600–800 ps. This time scale, when inserted in a continuum model expression along with the values of ϵ_0 and ϵ_∞ , produces longitudinal relaxation time scales for dipole solvation in the range of half a nanosecond.^{63,64} This time scale is strikingly similar to what has been observed in numerous solvation dynamics experiments in AOT/water/heptane reverse micelles.^{2–10} As already discussed in the Introduction, these slow solvent time scales are expected to substantially slow down the TICT reaction rate in these confined environments. Note that the values of ϵ_0 at different pool sizes given in Table 1 represent the static permittivity of the microemulsion but *not* the static permittivity of water in the system. Also, ϵ_∞ not only comprises contributions from polarizability but also contains contributions from more bulk-like water in the center of the pools. This is the reason for the strong rise of ϵ_∞ with the increase in pool size. However, the polarity of water in the pool can be given by the dispersion amplitude, $\Delta\epsilon = \epsilon_0 - \epsilon_\infty$. Assuming now that all water in the system contributes to this dispersion (which is, of course, not completely true), the static dielectric constant at a given pool can be roughly estimated as follows: $\epsilon_0(w_0) \approx 3 + \Delta\epsilon(w_0) \times C_W(100)/C_W(w_0)$, where $C_W(100)$ and $C_W(w_0)$ are the molar concentrations of pure water and water at a given w_0 , respectively. Using this relation, the estimated values for the “true” ϵ_0 for confined water at w_0 values of 20, 30, and 40 become 16, 12, and 17, respectively. These values, although smaller than those obtained from the peak shift studies, now compare reasonably with the data presented in Figure 1. The following could be the possible reasons for this: (i) the surfactant concentration is larger (0.5 M) for permittivity studies than that (0.1 M) used for emission studies, (ii) a very approximate method used for the estimate, and (iii) while in emission studies, the probe senses the “average” polarity of the environment constituted by both the “bound” and “free” water molecules inside the reverse micelles and also the interactions due to the ions; only the water molecules that are mobile (“free”) or partially free contribute to the dielectric relaxation. Therefore, every component in the confined pool contributes to the average polarity and hence influences the yield of a reaction (static effects), whereas only the relatively free dipolar molecules participate in the dynamical solvent control via the orientational relaxation.

TABLE 1: Dielectric Relaxation Data as Obtained from the Permittivity Measurements at Different Pool Sizes (w_0) in AOT/Water/Heptane Reverse Micelles with AOT Concentration at 0.5 M^a

[AOT] (M)	w_0	ϵ_0	τ (ps)	β	ϵ_∞	$\Delta\epsilon = \epsilon_0 - \epsilon_\infty$	χ^2_{CD}	χ^2_D
0.50	10	7.453	866.0	0.9493	4.329	3.124	0.0143	0.0210
0.50	20	7.940	639.4	0.7703	5.634	2.306	0.0098	0.0144
0.50	30	9.401	501.3	0.8591	6.846	2.555	0.0139	0.0085
0.50	40	13.59	678.6	0.7730	8.574	5.016	0.0173	0.0142

^a Here, ϵ_0 and ϵ_∞ respectively denote the static and infinite frequency dielectric constants of the droplets, τ is the relaxation time responsible for the dispersion ($\epsilon_0 - \epsilon_\infty$), and β is the coefficient associated with the distribution of environment in the Cole–Davidson description of orientational relaxation. χ^2_{CD} and χ^2_D are the reduced error for the corresponding Cole–Davidson and simple Debye fits (with the same parameter values as with CD) to the data.

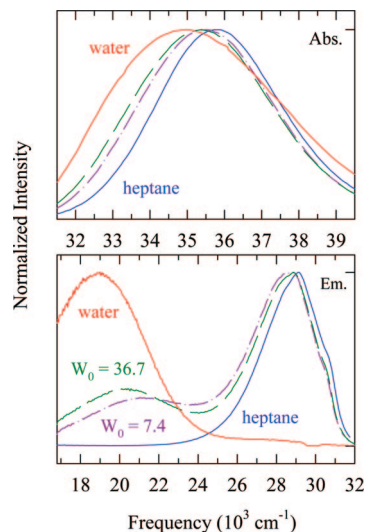


Figure 2. Representative absorption (upper panel) and emission (lower panel) spectra of the TICT molecule M6C at two different values of w_0 as well as those in heptane (blue) and water (red). The spectra at $w_0 = 7.4$ are denoted by dashed–dotted lines (pink), and those at $w_0 = 36.7$ are denoted by dashed lines (dark green).

C. TICT Reaction in AOT/Water/Heptane Reverse Micelles: Steady-State Fluorescence Study. Representative absorption and emission spectra of M6C in reverse micelles at two different pool sizes and those in water and heptane are shown in Figure 2. Relative to M6C in heptane, the broadening as well as red-shift in the absorption spectra in reverse micelles (upper panel, Figure 2) clearly indicate that the solute (M6C) molecule is interacting with the polar environment inside these microemulsions. The absorption spectrum in water, however, shows the maximum broadening and largest shift due to larger solvent polarity ($\epsilon_0 \approx 80$). The emission spectra shown in the lower panel (Figure 2) indicate that the CT population increases as the pool size becomes larger. This is consistent with the data shown in Figure 1, where the estimated average polarity of the confined pool is found to increase with the pool size (w_0). The emission spectra also seems to suggest that the LE \rightarrow CT conversion reaction for M6C takes place almost irreversibly in water, whereas the formation of CT is strongly disfavored in heptane. Also, there is a possibility that being soluble in heptane, M6C could also be partitioned into the heptane and micellar pseudophases and the two peaks in the emission profile might correspond to the emissions from these two different environments.^{35,40} However, the difference between these two peaks is $\sim 8000 \text{ cm}^{-1}$, which is too large a shift for M6C to be caused by the polarity of the confined solvent pool. This is further supported by the emission spectra of M6C in bulk solvents with different values of ϵ_0 (Figure S5, Supporting Information). Therefore, the emission spectra of M6C in reverse micelles shown in Figure 2 are indeed representing emissions from the

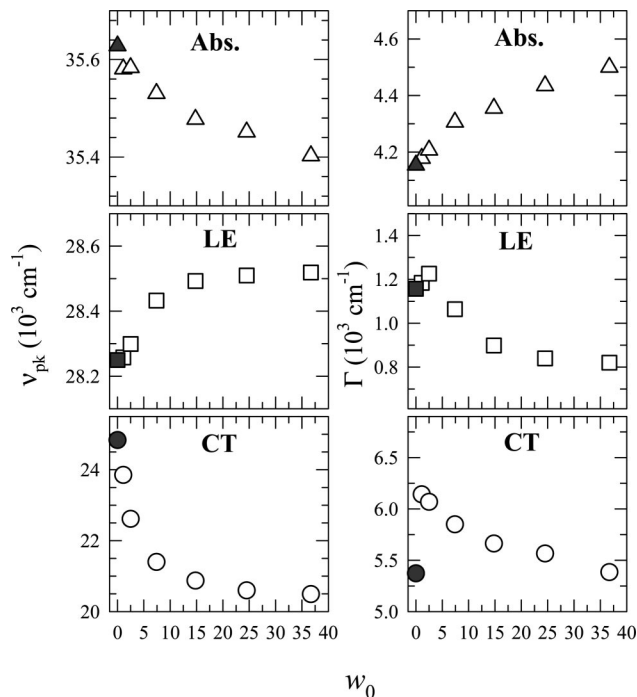


Figure 3. Spectral peak frequencies (ν_{pk} , left panels) and bandwidths (Γ , right panels) of M6C in AOT/water/heptane reverse micelles at different values of w_0 . The filled symbols (gray) denote the values of these spectral quantities at $w_0 \approx 0$. Note that, for the LE and CT emission bands, the widths (Γ) represent the inhomogeneous widths.

LE and CT states of the photoexcited molecule dissolved in the confined solvent pool.

The pool size dependence of spectral peak frequency and bandwidth of M6C is shown in Figure 3, where the values at “zero” water concentration are also shown (filled symbols). As expected, the absorption peak frequency (left-upper panel) shifts toward lower energy by $\sim 200 \text{ cm}^{-1}$ as the pool size swells up by a factor of ~ 33 . The absorption bandwidth (right-upper panel) also broadens by similar amount. Note that the red-shift in absorption spectrum with concomitant broadening with solvent polarity has also been observed previously for other ICT molecules and nonreactive probes in a number of different solution environments. The peak frequency for the LE emission band (left-middle panel) shows a blue-shift with the increase in w_0 , which is counterintuitive because the increase in average polarity with w_0 is expected to shift the LE band toward lower energy.^{45,46} Even though the total LE shift observed in the whole range of w_0 is merely 250 cm^{-1} , the systematic nature of the variation may be real, and we do not know the reasons for such a behavior. The pool size dependencies of the CT emission peak frequency and bandwidth are shown in the lower panels of Figure 3. Note here that the CT emission peak frequency at the first nonzero value of w_0 (that is, $w_0 = 1.1$) is about 4500 cm^{-1}

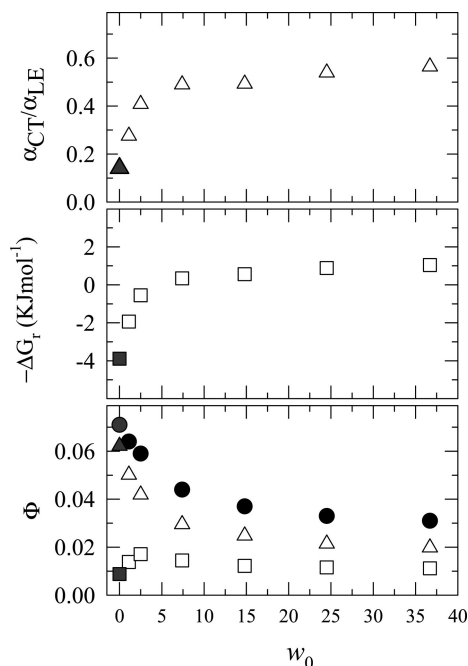


Figure 4. The ratio between the areas under the CT and LE emission bands (α_{CT}/α_{LE}), the change in reaction free energy ($-\Delta G_r$) associated with the $LE \rightarrow CT$ conversion and quantum yield (Φ) for M6C are shown as a function of w_0 . For further discussion, see text.

red-shifted from the LE peak frequency of M6C in heptane. This suggests that M6C is indeed interacting with the polar environment of the reverse micelles. Also, the CT band shows a red-shift of approximately 4000 cm^{-1} for changing w_0 from ~ 1 to ~ 37 and accompanies total narrowing of the bandwidth (inhomogeneous) of about 750 cm^{-1} . The large amount of red-shift in the CT band indicates stronger solute–solvent polar interactions in the bigger solvent pools. The large value of the bandwidth at $w_0 \approx 1$ indicates strong heterogeneity in the environment around the reactant molecule. The bandwidth, however, decreases with w_0 , as the larger pool size leads to increased “homogenization” of the environment. Note that the polarity dependence of the CT emission peak frequency and bandwidth for M6C in reverse micelles via w_0 is also similar to those for a few TICT molecules in electrolyte solutions,⁵¹ and nonreactive solvation probes in neat solvents.⁴⁶

Next we turn our attention to the spectral properties observed in the microemulsions in the absence of any added water. More precisely, what does the values of peak frequencies (absorption and emission), bandwidths and other steady state properties (shown by the filled gray symbols) at $w_0 \approx 0$ mean? There is always a finite possibility that a trace amount of water could be present as an impurity in either heptane or in the surfactant (AOT is known to absorb moisture), or even in both, that would lead to the formation of a cavity with trapped water molecules in it. In such a scenario, the cavity radius may easily be in the range of $2\text{--}3\text{ \AA}$ (approximately the size of an oxygen atom). Since the van der Waals radius of M6C is $\sim 3.5\text{ \AA}$,⁴⁵ the cavity would be able to barely accommodate an M6C molecule. Consequently, the rotation of the donor moiety (the morpholenyl group in M6C) would be severely hindered as a result of the close proximity of the surfactant head groups to the molecule undergoing reaction in such a narrow pore. The effects of the low polarity and severe spatial restriction at $w_0 \approx 0$ are then likely to be manifested in several properties such as the stabilization energies (peak frequencies), formation of LE and CT populations, equilibrium constant and finally on the reaction

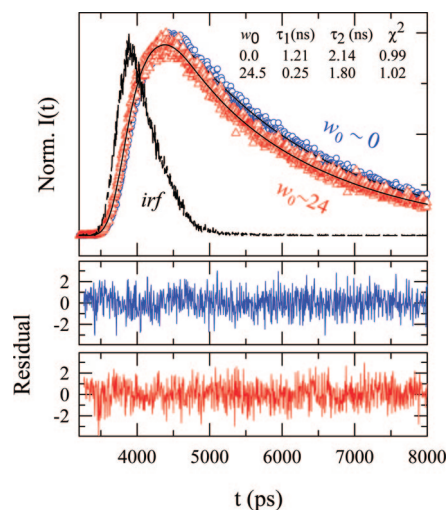


Figure 5. Representative time-resolved LE emission decays of M6C dissolved in AOT/water/heptane reverse micelles at two different pool sizes: $w_0 \approx 0$ (blue circles) and at $w_0 \approx 24$ (red triangles) along with time constants and χ^2 values obtained from biexponential fits (solid lines going through the symbols). The residuals (color-coded) for these pool sizes are shown in the lower panels. The amplitudes (a_1 and a_2) at $w_0 \approx 0$ and $w_0 \approx 24$ are (0.86, 0.14) and (0.71, 0.29), respectively. Note the LE emission decays were collected at wavelengths corresponding to the peak of the steady state emission spectra.

rate. Interestingly, the spectral properties obtained at $w_0 \approx 0$ are strongly related with those at other nonzero values of w_0 , suggesting that average polarity of the confined pool could indeed be a good correlating property for TICT reactions in such confined media. Note, however, that the CT bandwidth at $w_0 \approx 0$ is narrower by $\sim 750\text{ cm}^{-1}$ compared to that at $w_0 \approx 1$, and almost the same at $w_0 \approx 37$. The presence of very few water molecules in the cavity at $w_0 \approx 0$ cannot form multiple solvation layers, and thus the extent of spatial heterogeneity in this pool size may not be large. This might be one of the probable reasons for the comparable bandwidths at these two extreme pool sizes.

The pool size (w_0) dependence of the CT/LE area ratio (α_{CT}/α_{LE}) for M6C in reverse micelles is presented in Figure 4 (upper panel). The area under each band (α_x , $x = CT$ or LE) has been calculated as discussed previously.⁴⁵ Note here that the CT/LE ratio increases as the pool size becomes larger. This suggests that the formation of the CT state is increasingly favored as w_0 grows larger with successive addition of water at a fixed surfactant concentration. Note that the area ratio (α_{CT}/α_{LE}) is 4 times larger at $w_0 \approx 37$ than that at $w_0 \approx 0$. The fact that the CT population is $\sim 10\%$ at $w_0 \approx 0$ and none in heptane suggests that M6C is located either at the polar interface of the microemulsion or partially encapsulated inside the cavity. We would like to mention here that the LE population also derives contribution from those M6C molecules that may be partitioned into the heptane phase.^{35,40} As the formation of CT population is severely inhibited in nonpolar solvents such as heptane, the growth of the CT/LE ratio with w_0 is directly linked to the average polarity (ϵ_0) of the solvent pool encapsulated in these reverse micelles. The average polarity of the pool, however, cannot entirely control the formation of the CT state as the confinement exerts restriction on the rotation of the donor group (morpholenyl group in M6C). The extra restriction arises from the enhanced rigidity of the solvent molecules due to confinement. The effects of the environmental rigidity is best understood when the CT/LE area ratio at a particular w_0 is compared with that in bulk solvents with comparable dielectric constant.

For example, the ratio (α_{CT}/α_{LE}) at $w_0 \approx 37$ is 0.56, whereas it is ~ 15 in bulk propanol ($\epsilon_0 \approx 20.5$).⁶⁹ Therefore, in a polar pool with comparable ϵ_0 , the area ratio for M6C is almost 27 times less than that in bulk propanol.⁶⁹ As the area ratio is connected to the equilibrium constant (K_{eq}) for the $LE \rightarrow CT$ conversion reaction in M6C, this reduction in area ratio is translated to a lowering of K_{eq} by a factor of ~ 14 at $w_0 \approx 37$. Subsequently, the change in reaction free energy ($-\Delta G_r$) associated with the conversion reaction is calculated by using the relation

$$-\Delta G_r = RT \ln K_{eq} = RT \ln [\alpha_{CT} \nu_{LE}^3 / \alpha_{LE} \nu_{CT}^3] \quad (3)$$

and shown as a function of pool size in the middle panel of Figure 4. As expected, $-\Delta G_r$ is following the trend of α_{CT}/α_{LE} depicted in the upper panel of Figure 4. Note that the pool-size-dependent $-\Delta G_r$ varies from negative to positive values, indicating that an unfavorable $LE \rightarrow CT$ conversion reaction in smaller pool sizes becomes favorable in bigger microemulsion droplets. In fact, the equilibrium constant is ~ 7 times larger at $w_0 \approx 37$ than that at $w_0 \approx 0$. Note also that $-\Delta G_r$ at $w_0 \approx 37$ is approximately 7 times smaller than that in the bulk propanol, suggesting a substantial slowing down of the reaction upon confinement.

We have estimated quantum yield, radiative and nonradiative rates, and transition moments for M6C in all pool sizes. The following relation has been used to determine the quantum yield:⁴⁵

$$\Phi = \Phi_R \left(\frac{n_S^2}{n_R^2} \right) \left(\frac{I_S}{I_R} \right) \left(\frac{1 - 10^{-0.5A_R}}{1 - 10^{-0.5A_S}} \right) \quad (4)$$

where n_x is the refractive index of the reference solution (R) and sample (S). For sample, the refractive indices are assumed to be the same as that of bulk water. I denotes the integrated emission intensity, and A is the absorbance. Quinine sulfate dihydrate in 0.05 M H_2SO_4 has been used as the reference ($\Phi_R = 0.508$).⁴⁵ Values of net quantum yields as well as those for LE and CT emission bands for M6C calculated by using eq 4 are shown in the lower panel of Figure 4. Note that both the net quantum yield and that associated with the LE band decrease as w_0 increases, whereas the quantum yield for the CT band initially increases and then saturates with w_0 . Interestingly, the pool size dependence of the quantum yields for M6C is similar to the electrolyte concentration dependence for several related compounds in electrolyte solutions studied earlier.^{50,51} A partial restoration of the three-dimensional H-bond network at higher w_0 values is probably the reason for the observed decrease, since extensive H-bond network in water is known to augment the nonradiative relaxation channels. A recent study of TICT reaction in water–tertiary butanol (water–TBA) mixtures has also indicated that partial destruction of the H-bond network of water at higher TBA concentration leads to the increase in net quantum yield.⁵⁰ The net quantum yield of M6C at $w_0 \approx 37$ is also found to be similar to those ($\sim 0.045 \pm 0.01$) in some moderately polar bulk solvents such as ethyl acetate ($\epsilon_0 = 6.02$) and tetrahydrofuran ($\epsilon_0 = 7.58$).⁷⁰

The radiative (k_{LE}^{rad}) rate has been determined by using the following relation:⁴⁵ $k_{LE}^{rad} = \phi_{LE}/\langle \tau_{LE} \rangle$, where the average LE lifetime has been calculated from the amplitudes (a_i) and time constants (τ_i) obtained by fitting the relevant LE emission decays (shown later in Figure 6) as follows: $\langle \tau_{LE} \rangle = \sum_i a_i \tau_i / \sum_i a_i$. The nonradiative rate for LE (k_{LE}^{nr}) is then calculated by using the relation⁴⁵ $k_{LE}^{nr} = (1 - \phi_{LE})/\langle \tau_{LE} \rangle$. These quantities have been calculated at several values of w_0 and are summarized in Table

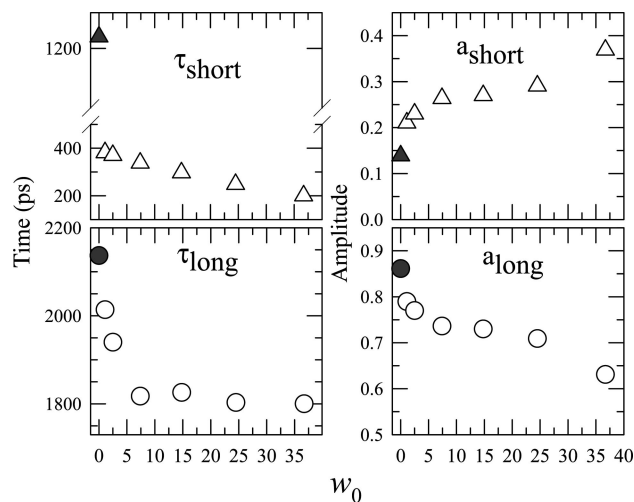


Figure 6. Time constants (τ_i , i = short or long) and amplitudes (a_i) obtained after fitting the LE emission decays with biexponential function of time at different pool sizes (w_0). τ_{short} is assumed to be the reaction time (τ_{rxn}) for the $LE \rightarrow CT$ conversion reaction in M6C.

TABLE 2: Pool Size (w_0)-Dependent Radiative, Nonradiative, and Absorption Transition Moments of M6C AOT/Water/Heptane Reverse Micelles

w_0	$K_{LE}^{rad} (10^7 s^{-1})$	$K_{LE}^{nr} (10^9 s^{-1})$	$M_{abs} (D)$
0.0	3.097	0.467	3.6
1.1	3.003	0.569	3.5
2.5	2.653	0.607	3.2
7.4	2.067	0.680	3.6
14.8	1.754	0.690	3.3
24.5	1.587	0.724	3.6
36.7	1.531	0.757	3.8

2. The error bar associated with the calculation of these radiative and nonradiative rates is typically $\pm 15\%$ about the values reported here. Since CT quantum yield is very small (lower panel, Figure 4), the radiative rate for the CT emission band has not been calculated. Data in Table 2 indicate that, while the radiative rate (k_{LE}^{rad}) decreases with w_0 , the nonradiative rate (k_{LE}^{nr}) increases with the pool size. The net absorption transition moments of the composite absorption band ($S_0 \rightarrow L_a + S_0 \rightarrow L_b$) is calculated as follows:⁴⁵

$$M_{abs}/D = 9.584 \times 10^{-2} \left[\frac{1}{n_{abs}} \int (\epsilon(\nu)/M^{-1}cm^{-1}) \frac{d\nu}{\nu} \right]^{1/2} \quad (5)$$

where $\epsilon(\nu)$ is the molar decadic extinction coefficient. The results obtained by using eq 5 for M6C at various values of w_0 are shown in Table 2, and the error bar associated with the calculation is $\pm 15\%$ (of the reported value). It is evident from this table that these absorption transition moments do not show any dependence on pool size, which was also found for several TICT molecules in neat solvents,⁴⁵ electrolyte solutions,^{51,52} and water–TBA mixtures at higher alcohol mole fractions.⁵⁰

D. Time-Resolved Studies of TICT Reaction in Reverse Micelles: Pool Size Dependence. The TICT reaction in M6C has been studied in seven different pool sizes to investigate the pool size dependence of the reaction rate and its relation to the slow orientational relaxation time observed in the dielectric relaxation experiments. As already mentioned in the Introduction, emission decays of M6C in all pool sizes have been found to be biexponential with time. This is rather interesting because, with solvent dynamics being sluggish in confined environments, the reaction is expected to not be in the rapid solvent equilibration limit.⁴⁵ This would then lead to a deviation from the

biexponential character of the time-resolved emission intensity decay, questioning the validity of the classical two-state reversible reaction mechanism as described previously.⁴⁵ Also, because of the microscopic heterogeneity both in the solvent structure and dynamics as well as the solute distribution, a stretched exponential rather than a simple biexponential function is expected to properly describe the decay kinetics. The fact that a time dependent biexponential function can sufficiently describe the decay kinetics in reverse micelles is probably a reflection of the recently discovered ultrafast motions of the water molecules in AOT reverse micelles.²⁶ As the reactive motion in the TICT framework involves rotation (twisting) of the donating group, the friction it experiences is largely dictated by the molecular length scale processes and hence coupled to the nearest-neighbor solvent spatial correlations.⁶³ In such a length scale, the dynamical solvent modes are governed by the slow solvent orientational and translational motions.^{63,64} However, if the initial solvent response is extremely rapid with large amplitude, then the ultrafast solvent modes can bring back the reaction significantly close to the rapid solvent equilibrium limit. This may be the reason for the observed biexponential decay of the time-resolved intensity emission decays in the reverse micelles at different pool sizes. It may also be that the broader time resolution (~ 475 ps) employed in this study has led to the absence of the faster time scales, and consequently the decay appears to be biexponential in time.

Representative biexponential fits to the emission decays collected at peak wavelength of LE at $w_0 \approx 0$ and $w_0 \approx 24$ are shown in Figure 5, where fit parameters are also summarized. Clearly, the LE emission decays are biexponential with time, as the residuals do not contain any nonrandom pattern, and values for the “goodness of fit parameter” (χ^2) are close to 1. While the shorter one between the two time constants obtained by fitting the LE emission decays at a given pool size is believed to be associated with the reaction time of the LE \rightarrow CT conversion reaction in M6C, the longer time constant reflects the average time for LE decay to the ground state. Note that the values of the longer time constant (2.1 and 1.8 ns) at these two pool sizes are similar to those found for another closely related TICT molecule, 4-(1-azetidynyl)-benzonitrile (P4C) in TBA-water solutions at higher TBA mole fractions.⁵⁰ The reaction time for the LE \rightarrow CT conversion reaction in M6C is ~ 250 ps at $w_0 \approx 24$ and ~ 1200 ps at $w_0 \approx 0$. Note here that an unconstrained biexponential fit to the CT emission decay at $w_0 \approx 24$ has also produced a rise time of 260 ± 20 ps and a long time constant of about 2 ns. These values are very similar to the time constants found for the LE emission decay collected at this pool size ($w_0 \approx 24$). This has also been observed in earlier studies with several closely related TICT molecules.^{45,50,52} The shorter time constant is indeed then the reaction time for M6C in these confined environments. Note here that, if the LE emission decay at $w_0 \approx 0$ is fitted to a single exponential, the fit worsens, generating nonrandom patterns at shorter times of the total decay profile. However, the fit becomes smoother and the residual more regular if a biexponential function of time is used. Interestingly therefore, the biexponential behavior of the decay kinetics for M6C in AOT/water/heptane reverse micelles also conform to the classical two-state reversible reaction mechanism as described by Maroncelli and co-workers in ref 45.

The biexponential fit parameters required to fit the LE emission decays of M6C at seven pool sizes are shown in Figure 6. Note that in the present study the fast time constant is simply the reaction time, as the decays are all biexponential with time.

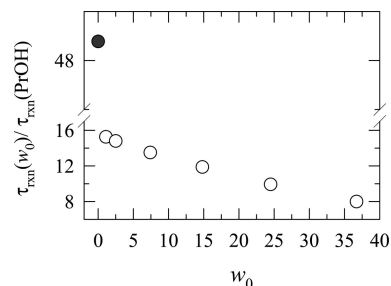


Figure 7. The ratio between the reaction time for M6C at a given pool ($\tau_{rxn}(w_0)$) and that in bulk propanol ($\tau_{rxn}(PrOH)$) is shown as a function of pool size, w_0 . For details, see text.

While the reaction times (τ_{short}) for M6C in reverse micelles obtained at different values of w_0 are presented in the left panels, the amplitudes are shown in the right panels of Figure 6. It is evident from the left-upper panel of Figure 6 that the reaction is 6 times faster at $w_0 \approx 37$ than that at $w_0 \approx 0$, with the amplitude of the shorter component (a_{short}) being ~ 3 times more at the largest pool than that at the smallest one. As the pool size grows bigger, the reaction time decreases simultaneously with the increase in amplitude of the associated component (a_{short}). The growth of the short component (a_{short}) with pool size suggests that the reaction is becoming favorable due to larger change in reaction free energy ($-\Delta G_r \propto \ln[a_{short}/a_{long}]$). Therefore, the pool size (w_0) dependencies of both the reaction time and amplitude clearly reflect that the reaction is increasingly favored as a result of enhanced polarity and better mobility of the environment as the pool grows in size. Note that the reaction time at the largest pool is ~ 200 ps and is strikingly close to that (~ 190 ps) of P6C in bulk decanol ($\epsilon_0 = 7.2$) at room temperature. This similarity in reaction times indicates that probably both the environment rigidity (via viscosity) and average polarity play important roles for determining the rates of such reactions in a given environment.

The reaction times shown in Figure 6 for w_0 values ranging from ~ 1 to ~ 37 are on the order of few hundreds of picoseconds, which are many times larger than that at bulk solvents of comparable polarities. For example, the LE \rightarrow CT conversion reaction for M6C in propanol at room temperature proceeds with a reaction time of approximately 25 ps, which is also similar to that obtained for P6C in the same solvent at similar condition.⁴⁵ The ratio between the reaction rate in reverse micelles and that in bulk propanol is shown as a function of pool size in Figure 7. The slowing down of the reaction rate by a factor of 10–20 between w_0 values ~ 1 to ~ 37 is partially linked to the slow orientational relaxation time scales of encapsulated water molecules in these reverse micelles. The reduced polarity of the solvent pool also contributes significantly to the slowing down of the formation of the CT state. Note that the data summarized in Table 1 lead to a longitudinal relaxation time scale (τ_L) in the range of 500 ps for dipolar solvation dynamics in AOT/water reverse micelles. It is therefore likely that the observed slow reaction times are a manifestation of slow solvent stabilization of the activated species as well as that of the charge-transferred product. Since the cavity size is barely enough for partially accommodating the M6C molecule along with a few water molecules at $w_0 \approx 0$, the rotation of the donating moiety becomes severely restricted. Also, a drastic reduction in the average polarity in such a small cavity may not be able to sufficiently stabilize the CT state. Consequently, the reaction rate at $w_0 \approx 0$ becomes almost 50 times slower than that in bulk propanol.

IV. Conclusion

The main results of the paper are as follows. A new TICT molecule has been synthesized, and photophysics and photochemistry have been studied at several pool sizes in AOT/water/heptane reverse micelles. The net quantum yield of M6C is found to decrease as the pool size grows in size, whereas the nonradiative rate increases. The absorption transition moment remains insensitive to the pool size. The pool size dependencies of these photophysical quantities appear to be similar to the alcohol mole fraction dependence of a closely related TICT molecule in TBA–water mixtures at higher TBA concentrations.⁵⁰ This similarity suggests the role of the three-dimensional H-bond network structure of water in determining the photophysics of dissolved probes. The average static dielectric constants of the solvent pools have been estimated from the emission peak frequencies of a nonreactive probe dissolved in these microemulsions as well as from the permittivity measurements of reverse micelles using 0.5 M AOT. The estimated bulk dielectric constant in the confined environment is found to be drastically different from that of bulk water. The reduction in average polarity then leads to less production of the CT state in M6C upon photoexcitation. At the largest pool size ($w_0 \approx 37$), the equilibrium constant (K_{eq}) for the LE \rightarrow CT conversion reaction of M6C is found to be 15 times smaller than that in bulk propanol, whose polarity is comparable to the estimated polarity at this pool size. The change in reaction free energy ($-\Delta G_r$) are also found to be ~ 8 times smaller than that in bulk propanol. Interestingly, $-\Delta G_r$ changes sign (from negative to positive) with the increase in pool size, indicating that the reaction becomes more favorable at larger w_0 values.

The permittivity measurements have been carried out to estimate the orientational relaxation time scales at different pool sizes of these reverse micelles with 0.5 M AOT concentration. The relaxation time scales found in this study lie in the range of 600–800 ps. These time scales are interpreted as originating from the slow orientation of the water molecules near the interface and are also believed to be responsible for the slow component observed in the time-resolved Stokes shift experiments in confined aqueous media.^{1–10} The slow orientation of the solvent molecules is probably also responsible for the observed slowing down of the LE \rightarrow CT conversion reaction for M6C in these reverse micelles. The similarity between the dielectric relaxation time scales and the reaction times (200–400 ps) seems to provide further support to the assumed coupling between the slow solvent reorganization and TICT reaction in confined environments.

As the permittivity measurements were done at 0.5 M AOT concentration, we investigated the effects of surfactant concentration on the LE \rightarrow CT reaction of M6C at two representative pool sizes: $w_0 = 7.4$ and $w_0 = 24.5$. The steady-state studies indicate that at both the pool sizes the absorption and LE peak frequencies show red-shift by 400–600 cm^{-1} upon changing the AOT concentration from 0.1 to 0.5 M. However, the LE emission band is found to broaden by a similar amount. Interestingly, the CT shift is much smaller ($\sim 100 \text{ cm}^{-1}$) and accompanies narrowing by about 800 cm^{-1} for increasing the AOT concentration to 0.5 M. The narrowing of the CT band is the direct effect of the increasing solute–environment interaction⁴⁶ at higher AOT concentration. The increase in AOT concentration also enhances the CT population relative to that of LE, which leads to the enhancement of $-\Delta G_r$ by a factor of 6 at $w_0 = 7.4$ and ~ 4 at $w_0 = 24.5$ for changing the AOT concentration from 0.1 to 0.5 M. The reaction rate, on the other hand, slows down by $\sim 70\%$ at $w_0 = 7.4$ and $\sim 25\%$ at $w_0 =$

24.5 for increasing the concentration from 0.1 to 0.5 M. The stronger ion–dipole interactions leading to higher dielectric friction on the twisting mode as well as further reduced polarity at higher AOT concentration may be responsible for such a slowing down of the reaction rate. However, further studies with several other AOT concentrations and at different pool sizes are required to understand the surfactant concentration effects on such reactions.

Since these confined environments are known to possess strong spatial heterogeneity, the average reaction rate is expected to be significantly coupled to the location of the TICT molecule inside the confined solvent pool. For example, if the relatively stronger ion–dipole interaction makes the TICT molecule reside near the interface created by the AOT headgroup and polar solvent molecules, the reaction rate would be largely dictated by the time scale and polarity of that locality. On the other hand, if strong dielectric screening and proper solvation drive the reactant molecule to go into the center of the pool, the enhanced mobility and increased polarity would render the reaction more facile and faster. In principle, one can resolve the spatial heterogeneity of reaction rate by selectively exciting the population via excitation wavelength dependence study. Such a study on vibrational dynamics of confined water molecules has recently been carried out where a moderate dependence on excitation wavelength is indicated.^{25,26} Moreover, several recent studies^{1–10,16} have suggested the presence of a significant amount of ultrafast component in aqueous reverse micelles with a time constant in the range of 30–50 fs. One wonders then how the ultrafast response would scale with the spatial heterogeneity and what would be the effects of such ultrafast components on reactions that possess polar intermediates such as the TICT reaction? A coupled investigation of ultrafast solvation dynamics and reaction kinetics is therefore required to fully understand the environment effects on TICT reactions in these confined systems. A comparison among time scales measured in quaternary microemulsions,⁹ lecithin vesicles,¹⁶ catanionic⁴² and AOT/water/heptane reverse micelles^{2–10} suggests that solvent dynamics seems to be the fastest in the quaternary microemulsions and lecithin vesicles, and then sequentially comes catanionic and AOT/water/heptane reverse micelles. It would then be interesting to study whether a TICT reaction picks up the dynamical modes so neatly and the reaction rate is modified accordingly. Dynamical solvent control of TICT reaction in other molecules that possess higher activation energies in these confined environments might also be interesting.

Acknowledgment. R. Biswas thanks Professor S. K. Chattopadhyay, Kalyani University, for his help in synthesizing the M6C molecule and Professor M. Maroncelli, Pennsylvania State University, for kind support and encouragement. Anonymous reviewers are thanked for constructive criticisms and useful suggestions. Generous research grants from the Council of Scientific and Industrial Research (CSIR), India, and the Department of Science and Technology (DST), India, are gratefully acknowledged. T.P. thanks the University Grants Commission (UGC), India, for a research fellowship.

Supporting Information Available: Representative emission spectra of C153 in AOT/water/heptane reverse micelles, pool-size-dependent specific conductivities at two different AOT concentrations (0.5 and 0.1 M), and dielectric dispersion data at several pool sizes and emission spectra of M6C in a few bulk solvents. This material is available free of charge via the Internet at <http://pubs.acs.org>.

References and Notes

- (1) Levinger, N. E. *Science* **2002**, 298, 1722.
- (2) Bhattacharyya, K. *Acc. Chem. Res.* **2003**, 36, 95, and references therein.
- (3) Ghosh, S.; Mandal, U.; Adhikari, A.; Dey, S.; Bhattacharyya, K. *Int. Rev. Phys. Chem.* **2007**, 26, 421.
- (4) Luisi, P. L.; Straub, B. E. Eds. *Reverse Micelles: Biological and Technological Relevance to Amphiphilic Structures in Apolar Media*; Plenum: New York, 1984.
- (5) De, T.; Maitra, A. *Adv. Colloid Interface Sci.* **1995**, 59, 95.
- (6) Baruah, B.; Roden, J. M.; Sedgwick, M.; Correa, N. M.; Crans, D. C.; Levinger, N. E. *J. Am. Chem. Soc.* **2006**, 128, 12758.
- (7) Willard, D. M.; Riter, R. E.; Levinger, N. E. *J. Am. Chem. Soc.* **1998**, 120, 4151.
- (8) Harpham, M. R.; Ladanyi, B.; Levinger, N. E. *J. Phys. Chem. B* **2005**, 109, 16891.
- (9) Corbeil, E. M.; Levinger, N. E. *Langmuir* **2003**, 19, 7264.
- (10) Correa, N. M.; Levinger, N. E. *J. Phys. Chem. B* **2006**, 110, 13050.
- (11) Rosenfeld, D. E.; Schmuttenmaer, C. A. *J. Phys. Chem. B* **2006**, 110, 14309.
- (12) Vanables, D. S.; Huang, K.; Schmuttenmaer, C. A. *J. Phys. Chem. B* **2001**, 105, 9132.
- (13) Boyd, J. E.; Briskman, A.; Sayes, C. M.; Mittelman, D. A.; Colvin, V. J. *J. Phys. Chem. B* **2002**, 106, 6346.
- (14) Boyd, J. E.; Briskman, A.; Colvin, V. L.; Mittelman, D. M. *Phys. Rev. Lett.* **2001**, 87, 147401/1.
- (15) Zhong, Q.; Steinburst, D. A.; Carpenter, E. E.; Owrutsky, J. C. *Langmuir* **2002**, 18, 7401.
- (16) Bursing, H.; Ouw, S.; Kundu, P.; Vohringer, P. *Phys. Chem. Chem. Phys.* **2001**, 3, 2378.
- (17) Pileni, M. P. Ed. *Structure and Reactivity in Reverse Micelles*; Elsevier: Amsterdam, 1989; Vol. 65.
- (18) Cho, C. H.; Chung, M.; Lee, J.; Nguyen, T.; Singh, S.; Vedamuthu, M.; Yao, S.; Zhu, S. B.; Robinson, G. W. *J. Phys. Chem.* **1995**, 99, 7806.
- (19) Lundgren, J. S.; Heitz, M. P.; Bright, F. V. *Anal. Chem.* **1995**, 67, 3775.
- (20) Das, S.; Datta, A.; Bhattacharyya, K. *J. Phys. Chem. A* **1999**, 101, 3299.
- (21) Sarkar, N.; Das, K.; Datta, A.; Das, S.; Bhattacharyya, K. *J. Phys. Chem.* **1996**, 100, 10523.
- (22) Datta, A.; Mandal, D.; Pal, S. K.; Bhattacharyya, K. *J. Phys. Chem. B* **1997**, 101, 10221.
- (23) Riter, R. E.; Willard, D. M.; Levinger, N. E. *J. Phys. Chem. B* **1998**, 102, 2705.
- (24) Moilanen, D. E.; Levinger, N. E.; Spry, D. B.; Fayer, M. D. *J. Am. Chem. Soc.* **2007**, 129, 14311.
- (25) Tan, H.-S.; Piletic, I. R.; Fayer, M. D. *J. Chem. Phys.* **2005**, 122, 174501.
- (26) Piletic, I. R.; Tan, H.-S.; Fayer, M. D. *J. Phys. Chem. B* **2005**, 109, 21273.
- (27) Faeder, J.; Ladanyi, B. M. *J. Phys. Chem. B* **2001**, 105, 11148.
- (28) Faeder, J.; Ladanyi, B. M. *J. Phys. Chem. B* **2000**, 104, 1033.
- (29) Bhattacharyya, K.; Bagchi, B. *J. Phys. Chem. A* **2000**, 104, 10603.
- (30) Salaniwal, S.; Cui, S. T.; Cochran, H. D.; Cummings, P. T. *Langmuir* **2001**, 17, 1773.
- (31) Salaniwal, S.; Cui, S. T.; Cochran, H. D.; Cummings, P. T. *Langmuir* **2001**, 17, 1784.
- (32) Salaniwal, S.; Cui, S. T.; Cochran, H. D.; Cummings, P. T. *Langmuir* **1999**, 15, 5188.
- (33) Senapati, S.; Keiper, J. M.; DeSimone, J. M.; Wignall, G. D.; Melnichenko, Y. B.; Frielinghaus, H.; Berkowitz, M. L. *Langmuir* **2002**, 18, 7371.
- (34) Mahiuddin, S.; Renoncourt, A.; Bauduin, P.; Touraud, D.; Kunz, W. *Langmuir* **2005**, 21, 5259.
- (35) Silber, J. J.; Biasutti, A.; Abuin, E.; Lissi, E. *Adv. Colloid Interface Sci.* **1999**, 82, 189.
- (36) Falcone, R. D.; Correa, N. M.; Biasutti, M. A.; Silber, J. J. *Langmuir* **2002**, 18, 2039.
- (37) Falcone, R. D.; Correa, N. M.; Biasutti, M. A.; Silber, J. J. *J. Colloid Interface Sci.* **2006**, 296, 356.
- (38) Falcone, R. D.; Biasutti, M. A.; Correa, N. M.; Silber, J. J.; Lissi, E.; Abuin, E. *Langmuir* **2004**, 20, 5732.
- (39) Silber, J. J.; Falcone, R. D.; Correa, N. M.; Biasutti, M. A.; Abuin, E.; Lissi, E.; Campodonico, P. *Langmuir* **2003**, 19, 2067.
- (40) Novaira, M.; Biasutti, M. A.; Silber, J. J.; Correa, N. M. *J. Phys. Chem. B* **2007**, 111, 748.
- (41) Novaira, M.; Moyano, F.; Biasutti, M. A.; Silber, J. J.; Correa, N. M. *Langmuir* **2008**, 24, 4637.
- (42) Biswas, R.; Das, A. R.; Pradhan, T.; Tourad, D.; Kunz, W.; Mahiuddin, S. *J. Phys. Chem. B* **2008**, 112, 6620.
- (43) Grabowski, Z. R.; Rotkiewicz, K.; Rettig, W. *Chem. Rev.* **2003**, 103, 3899.
- (44) Lippert, E.; Rettig, W.; Bonacic-Koutecky, V.; Heisel, F.; Mieche, J. A. *Adv. Chem. Phys.* **1987**, 68, 1.
- (45) Dahl, K.; Biswas, R.; Ito, N.; Maroncelli, M. *J. Phys. Chem. B* **2005**, 109, 1563.
- (46) Horng, M. L.; Gardecki, J. A.; Papazyan, A.; Maroncelli, M. *J. Phys. Chem.* **1995**, 99, 17311.
- (47) van der Zwan, G.; Hynes, J. T. *Chem. Phys.* **1991**, 152, 169.
- (48) Hicks, J.; Vandersall, M.; Babarogic, Z.; Eiselthal, K. B. *Chem. Phys. Lett.* **1985**, 116, 18.
- (49) Hicks, J.; Vandersall, M. T.; Sitzmann, E. V.; Eiselthal, K. B. *Chem. Phys. Lett.* **1987**, 135, 413.
- (50) Pradhan, T.; Ghoshal, P.; Biswas, R. *J. Phys. Chem. A* **2008**, 112, 915.
- (51) Pradhan, T.; Biswas, R. *J. Phys. Chem. A* **2007**, 111, 11514.
- (52) Pradhan, T.; Biswas, R. *J. Phys. Chem. A* **2007**, 111, 11524.
- (53) The CT emission decays could not be collected for all pool sizes because of the very low CT quantum yield.
- (54) Rettig, W. *J. Lumin.* **1980**, 26, 21.
- (55) Rettig, W. *J. Phys. Chem.* **1982**, 86, 1970.
- (56) Biswas, R.; Lewis, J. E.; Maroncelli, M. *Chem. Phys. Lett.* **1999**, 310, 485.
- (57) Lewis, J. E.; Biswas, R.; Robinson, A. G.; Maroncelli, M. *J. Phys. Chem. B* **2001**, 105, 3306.
- (58) Krishna, M. M. G. *J. Phys. Chem. A* **1999**, 103, 3589.
- (59) Buchner, R.; Barthel, J.; Stauber, J. *Chem. Phys. Lett.* **1997**, 306, 57.
- (60) Barthel, J.; Feuerlein, F.; Neueder, R.; Wachter, R. *J. Solution Chem.* **1980**, 9, 209.
- (61) Song, W.; Biswas, R.; Maroncelli, M. *J. Phys. Chem. A* **2000**, 104, 6924.
- (62) Senapati, S.; Chandra, A. *J. Phys. Chem. B* **2001**, 105, 5106.
- (63) Bagchi, B.; Biswas, R. *Adv. Chem. Phys.* **1999**, 109, 207.
- (64) Bagchi, B.; Chandra, A. *Adv. Chem. Phys.* **1991**, 80, 1.
- (65) Balasubramanian, S.; Bagchi, B. *J. Phys. Chem. B* **2001**, 105, 12529.
- (66) The best model is achieved with minimizing the standard error, χ^2 : $\chi^2 = 1/(2m - k) \sum_{i=1}^m [(\epsilon_{i,\text{exp}} - \epsilon_{i,\text{cal}})^2 - (\epsilon_{i,\text{exp}} - \epsilon_{i,\text{cal}})^2]$, where m is the number of experimental data, and k is the number of adjustable parameters. The estimated χ^2 values from the above equation are listed in Table 1.
- (67) Maroncelli, M. *J. Mol. Liq.* **1993**, 57, 1.
- (68) The water molecules responding to the measurements are either trapped inside the surfactant layers and experience hydrophobic hydration or have formed the "water pool" in the core of the reverse micelle. Another kind of water molecules are also present which are "sticking" to the anionic surfactant as a result of strong ion-dipole interaction. Naturally, these water molecules are dielectrically saturated and would not respond to the applied electric field.
- (69) See the tabulated values supplied along with Figure S5 in the Supporting Information.
- (70) The values for the net quantum yield of M6C in ethyl acetate and tetrahydrofuran respectively are (0.040 ± 0.05) and (0.042 ± 0.05) (unpublished data).